Published in final edited form as:

Proc Meet Acoust. 2018 November 5; 35(1): . doi:10.1121/2.0000950.

Impact of stone characteristics on cavitation in burst wave lithotripsy

C. Hunter, **B. Cunitz**, **B. Dunmire**, **M. Bailey**, **A. Randad**, **W. Kreider**

Center for Industrial and Medical Ultrasound, Applied Physics Laboratory, University of Washington, Seattle, Washington, UNITED STATES

A.D. Maxwell, **M.D. Sorensen**

Department of Urology, University of Washington School of Medicine, Seattle, Washington, UNITED STATES

J.C. Williams

Department of Anatomy and Cell Biology, Indiana University School of Medicine, Indianapolis, Indiana, UNITED STATES

Abstract

Non-invasive kidney stone treatments such as shock wave lithotripsy (SWL) and burst wave lithotripsy (BWL) rely on the delivery of pressure waves through tissue to the stone. In both SWL and BWL, the potential to hinder comminution by exciting cavitation proximal to the stone has been reported. To elucidate how different stones alter prefocal cavitation in BWL, different natural and synthetic stones were treated in vitro using a therapy transducer operating at 350 kHz (peak negative pressure 7 MPa, pulse length 20 cycles, pulse repetition frequency 10 Hz). Stones were held in a confined volume of water designed to mimic the geometry of a kidney calyx, with the water filtered and degassed to maintain conditions for which the cavitation threshold (in the absence of a stone) matches that from in vivo observations. Stone targeting and cavitation monitoring were performed via ultrasound imaging using a diagnostic probe aligned coaxially with the therapy transducer. Quantitative differences in the extent and location of cavitation activity were observed for different stone types—e.g., “softer” stones (natural and synthetic) that disintegrate into “dusty” fragments produced larger prefocal cavitation clouds. Future work will focus on correlation of such cavitation metrics with stone fragmentation.

1. INTRODUCTION

Shock wave lithotripsy (SWL) is a non-invasive treatment used clinically for over 30 years to break kidney stones by delivering pressure waves through tissue. The large tensile tail of shocks delivered in SWL can lead to the formation of clouds of cavitation bubbles in the kidney. Although such cavitation activity near the stone can contribute to stone comminution, excessive cavitation can also cause injury and even shield the stone from treatment by subsequent shock waves.[1] Burst wave lithotripsy (BWL) is a new non-invasive treatment that relies on delivery of tone bursts of ultrasound rather than shock waves.[2] Although BWL excites bubbles differently than SWL, cavitation activity is still an important aspect of BWL as an ultrasound-based treatment.

Because ultrasound (US) imaging probes can be readily integrated with BWL transducers, it is possible to visualize cavitation activity during treatments in real time as variable hyperechoic regions on B-mode images. In a study involving BWL exposures of pig kidneys in vivo, a threshold was identified above which sustained cavitation activity was readily apparent on B-mode images, beginning in the collecting space and growing proximally toward the transducer. Moreover, exposures above this threshold for sustained cavitation were directly correlated with hemorrhagic kidney injury.[3] In addition, such threshold behaviors have been studied in vitro in kidney phantoms using high-speed photography and US imaging.[4–5] These studies demonstrated that (a) in vivo threshold behaviors can be qualitatively simulated in phantoms with confined fluid spaces; (b) thresholds are quantitatively repeatable with careful control of water conditions, including the dissolved gas concentration; and (c) the presence of a stone in the phantom can change the threshold. Beyond cavitation thresholds, other studies have shown that kidney phantom configurations also impact stone fragmentation.[6]

Here we seek to build on previous work by using a controlled in vitro test configuration to investigate how different types of natural and synthetic stones affect cavitation behaviors. Based on simple image processing of B-mode ultrasound images, we develop simple metrics of cavitation activity and interpret these metrics with regard to stone fragmentation.

2. METHODS

A. EXPERIMENTAL TEST CONFIGURATION

BWL exposures were delivered using a 6-element transducer with a 350 kHz center frequency, a 85 mm aperture, and a 10 cm focal distance. The transducer possessed a central opening in which a P4–2 imaging probe (Philips Healthcare, Bothell, WA) was aligned coaxially with the therapy beam to assist in targeting of the stone and to monitor cavitation activity. The therapy beam was characterized by an ellipsoidal focal region with −6 dB dimensions of 35 mm along the acoustic axis and 5 mm transverse to the acoustic axis. The BWL transducer was oriented in a test tank with the therapy beam pointing vertically down toward a target stone, which was held in a confined volume of water in a polyvinyl chloride (PVC) phantom designed to mimic the geometry of a kidney calyx (Fig. 1). The water in the test tank and phantom was filtered and degassed to maintain conditions for which the cavitation threshold (in the absence of a stone) matches that from in vivo observations.[5]

BWL exposures lasting 30 seconds were delivered to 10 different natural and synthetic stone types (26 stones total) using parameters chosen to match those used in other preclinical studies: 350 kHz center frequency, 7 MPa peak negative pressure, 20 cycle pulse duration, and 10 Hz pulse repetition frequency. Treatments were monitored on B-mode images acquired with the P4–2 imaging probe connected to a Verasonics ultrasound engine (Kirkland, WA). Imaging was synchronized with the therapy such that one image frame was collected after each BWL pulse.

Initially all stones were soaked in filtered and degassed water for 48 hours before treatment, however cavitation levels were observed to be markedly larger than *in vivo* observations.

Additional stone hydration over the course of a total of 10 days resulted in a notable decrease in cavitation and was more representative of *in vivo* observations.

B. IMAGE PROCESSING

For each BWL exposure, captured B-mode image sequences were analyzed in Matlab (MathWorks, Natick, MA) to quantify cavitation activity. In each image sequence, two regions of interest (ROI) were defined for analysis. As depicted in Fig. 2, a baseline ROI was defined in the region below the stone to provide a measure of the background B-mode intensity for a given exposure, while an ROI for quantifying cavitation activity was defined in the fluid space above the stone. Using the maximum grayscale intensity in the first frame of the baseline ROI to define a threshold for each image sequence, the cavitation ROI was segmented to define supra-threshold pixels as representative of cavitation activity. Based on this segmentation strategy, the area and centroid of cavitation in each image frame were calculated. The area of the cavitation ROI used in this effort is 3596 pixels (3.4 cm^2), and normalized cavitation areas are presented as fractions of this area. Although it is typical to view B-mode images using some compression of grayscale intensities, the image processing strategy described above was applied to uncompressed B-mode image data to facilitate the definition of a clear threshold to represent cavitation.

3. RESULTS

A. CAVITATION METRICS

Cavitation area was calculated as a fraction of the total collecting space region of interest that contained cavitation. The centroid of cavitation activity was calculated as the axial distance from the stone surface, with positive distances toward the transducer. An example of both metrics is displayed for two stone types in Fig. 3. Note that no centroid position is shown for the BegoStone as the overall level of cavitation was too small to make this metric meaningful. It is notable that the two metrics appear to be correlated in that the cavitation tends to move proximal to the stone as the total area of cavitation increases. A typical interpretation of such behavior is that the increasing cavitation reflects the incident acoustic waves, thereby leading to higher tensile pressures (and concomitant cavitation activity) closer to the transducer.

For the purpose of reporting a single steady state value of cavitation area, the mean of the area over the last 20 seconds was calculated for each stone. This metric is displayed for each stone in Fig. 4, where stones of the same composition but from different patients are denoted with a numbered value. It was observed that more porous stones (e.g. U-30, struvite, carbapatite) produced larger amounts of cavitation than less porous stones (e.g. Bego, COM, crystal).

As noted in Methods, cavitation areas were quantified relative to an intensity threshold determined from the baseline ROI. For the analysis presented in Fig. 4, the threshold was set as the maximum value in this ROI. This approach was designed to account for differing overall intensity levels in each image sequence; however, this particular selection of threshold values is somewhat arbitrary. To examine the sensitivity of results to this selection,

the analysis was repeated with the threshold for each image sequence scaled by a factor of 2. Using the altered thresholds, each of the reported cavitation areas was reduced, as characterized by an average scaling factor of 0.77. This scaling factor was relatively consistent across all stones with a standard deviation of 0.08. Such consistency suggests that even though threshold selection can alter cavitation area values, the relative differences among stones are fairly robust to this choice. Note that to avoid issues with signal-to-noise, these statistics are calculated only for the 17 stones with a normalized cavitation area above 0.05.

B. STONE BREAKING

To understand the significance of the range of observed cavitation behaviors, fragmentation experiments with 5 artificial BegoStones stones (6 × 3.5 × 3.5 mm) were conducted at each of three dissolved gas concentrations of the fluid in the phantom calyx. These three conditions were chosen to approximate the range of cavitation activities observed for natural stones. As plotted in Fig. 5, stone breaking is reported as the mass fraction of fragments broken into sizes < 2 mm, with larger areas of cavitation within the phantom calyx corresponding to less stone comminution. These results show a large change in fragmentation effectiveness across the range of cavitation areas observed for different natural stones.

4. CONCLUSION

BWL treatments of a range of stone types were simulated in vitro using a phantom that mimics a kidney calyx with a confined fluid volume. B-mode ultrasound was used for targeting and monitoring of treatments and showed that the test configuration reliably simulated in vivo observations in which treatments above a threshold produce sustained cavitation in the fluid around the stone. Metrics based on simple image processing of B-mode images demonstrate that cavitation behaviors vary considerably with stone type; moreover, the range of variability appears significant with regard to stone breaking performance. This result is consistent with related modeling efforts that demonstrate the potential for cavitation proximal to the stone to cause significant shielding.[7] Ongoing work will seek to develop correlations among cavitation metrics and stone fragmentation, with an ultimate goal of providing a platform to study how BWL treatment parameters can be adapted to accommodate different cavitation behaviors. Such efforts will consider metrics based on B-mode images as well as alternatives that rely on Doppler signals.

ACKNOWLEDGMENTS

We acknowledge funding support from NIH through NIDDK P01-DK043881 and K01-DK104854.

REFERENCES

1. Bailey MR, Cleveland RO, Colonius T, Crum LA, Evan AP, Lingeman JE, McAteer JA, Sapozhnikov OA, Williams JC. Cavitation in shock wave lithotripsy: the critical role of bubble activity in stone breakage and kidney trauma. 2003 IEEE Ultrasonics Symposium 2003.

2. Maxwell AD, Cunitz BW, Kreider W, Sapozhnikov OA, Hsi RS, Harper JD, et al. Fragmentation of urinary calculi in vitro by burst wave lithotripsy. J. Urol, 2015, 193(1):338–344. [PubMed: 25111910]

3. May PC, Kreider W, Maxwell AD, Wang Y- N, Cunitz BW, Blomgren PM, Johnson CD, Park JSH, Bailey MR, Lee D, Harper JD, and Sorensen MD. Detection and evaluation of renal injury in burst wave lithotripsy using ultrasound and magnetic resonance imaging. J. Endourol, 2017, 31(8):786–792. [PubMed: 28521550]

4. Hunter C, Maxwell AD, Cunitz BW, Dunmire B, and Kreider W. Thresholds for sustained bubble cloud generation in burst wave lithotripsy. J. Acoust. Soc. Am, 2016, 140(4):3310.

5. Hunter C, Ahn JS, Kreider W, Maxwell AD, Cunitz BW, Wang Y- N, Dunmire B, Bailey MR, Harper JD, Sorensen MD. Evaluation of in vitro burst wave lithotripsy exposure conditions. In "Scientific Program of 35th World Congress of Endourology Program Book and Abstracts." Journal of Endourology, 31(S2), 2017, paper BRPRS4–20.

6. Ahn J, Kreider W, Hunter C, Zwaschka T, Bailey M, Sorensen M, Harper J, and Maxwell AD. Improving environmental and stone factors toward a more realistic in vitro lithotripsy model. J. Acoust. Soc. Am, 2017, 141(5):3673–3674.

7. Maeda K, Maxwell AD, Colonius T, Kreider W, and Bailey MR. Energy shielding by cavitation bubble clouds in burst wave lithotripsy. Submitted to J. Acoust. Soc. Am, 8 2018.

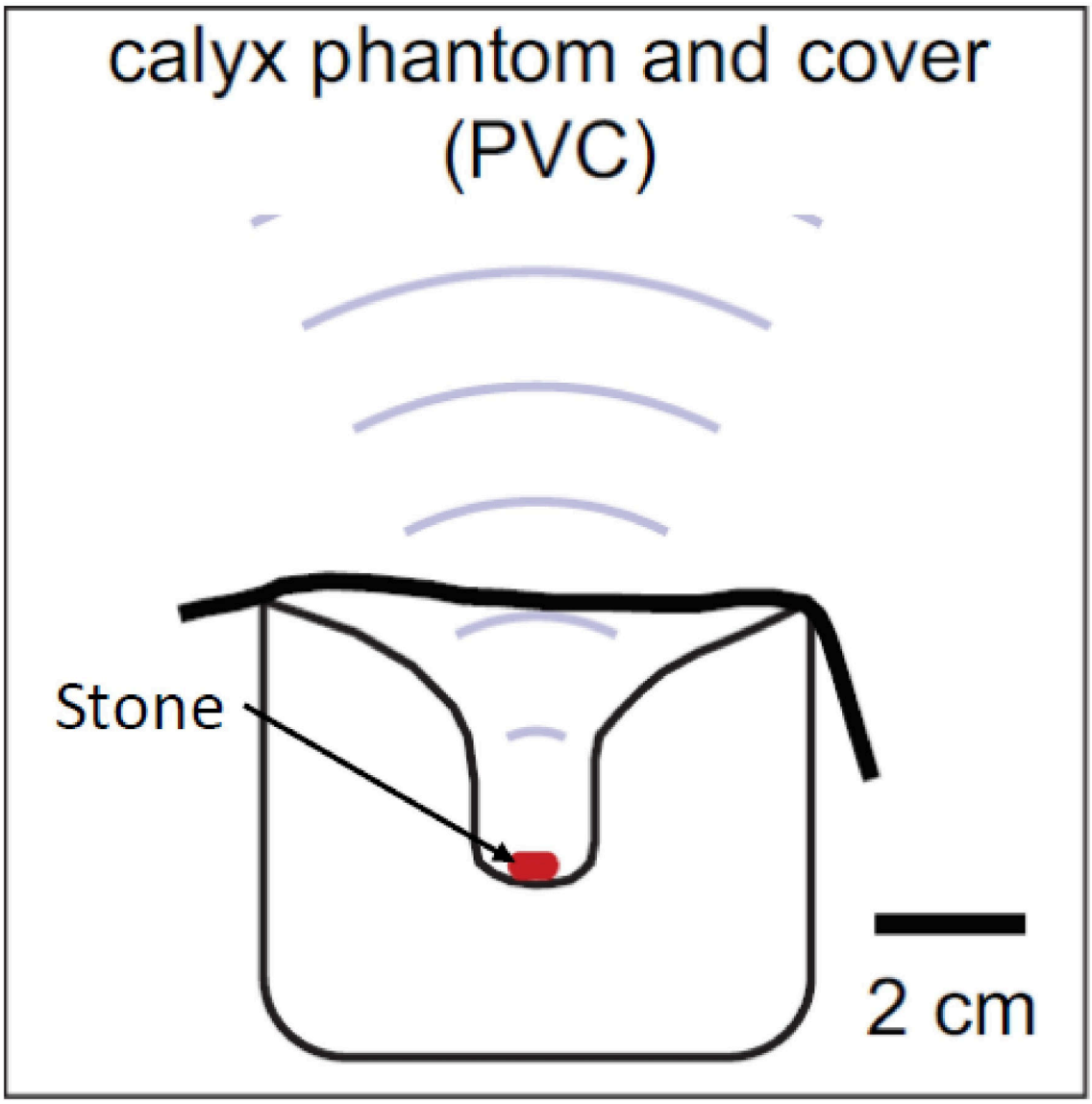

Figure 1:
Schematic of the experimental setup.

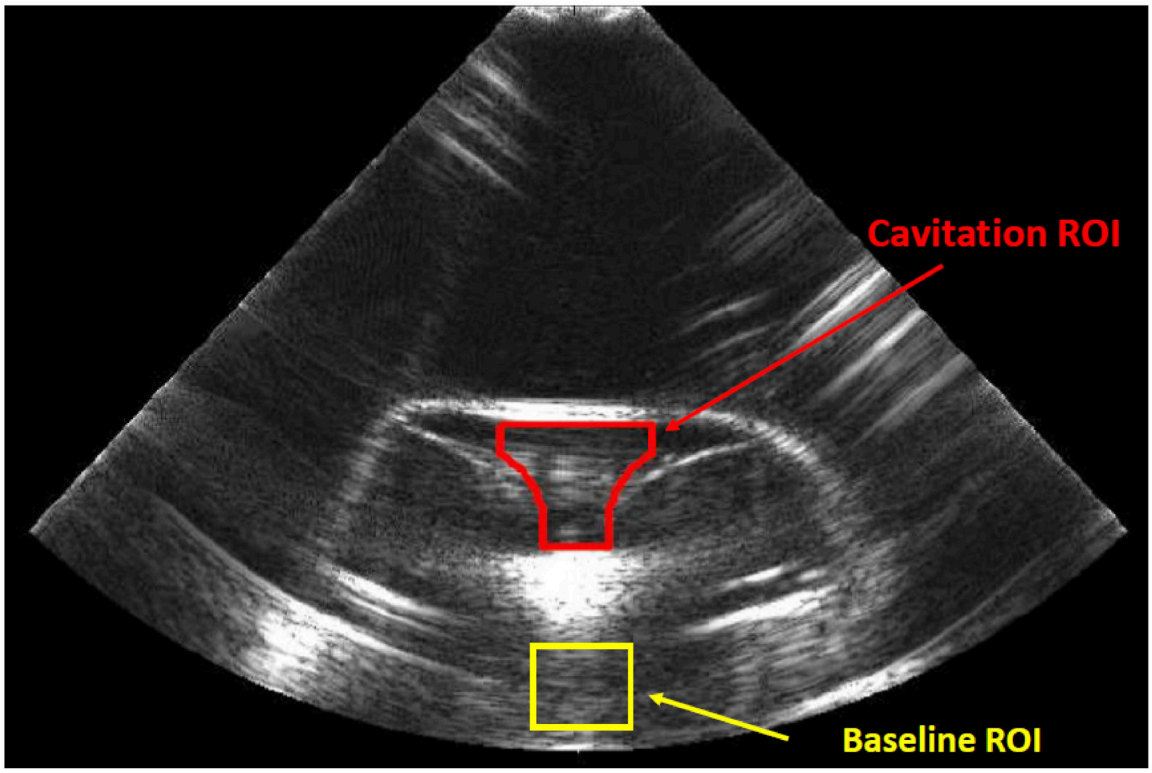

Figure 2:
Example B-mode image with regions of interest.

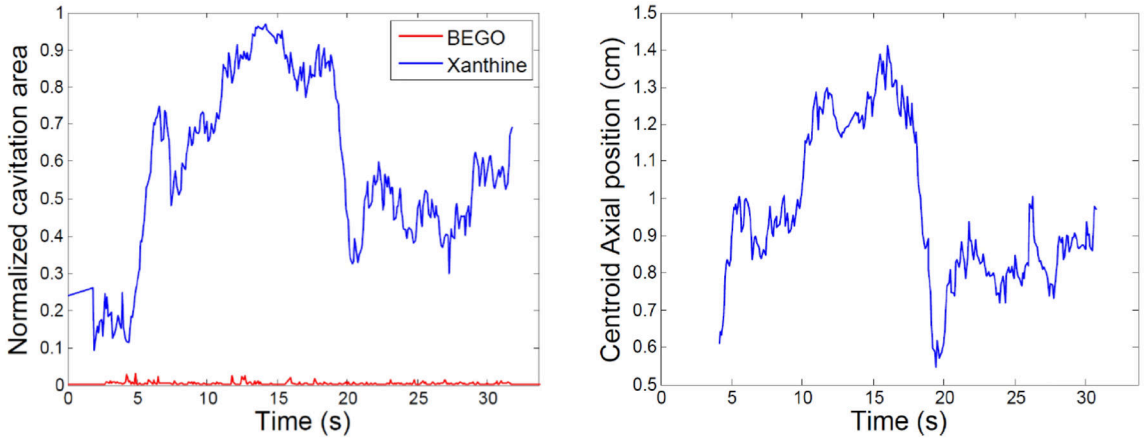

Figure 3:
Normalized cavitation area and axial centroid position.

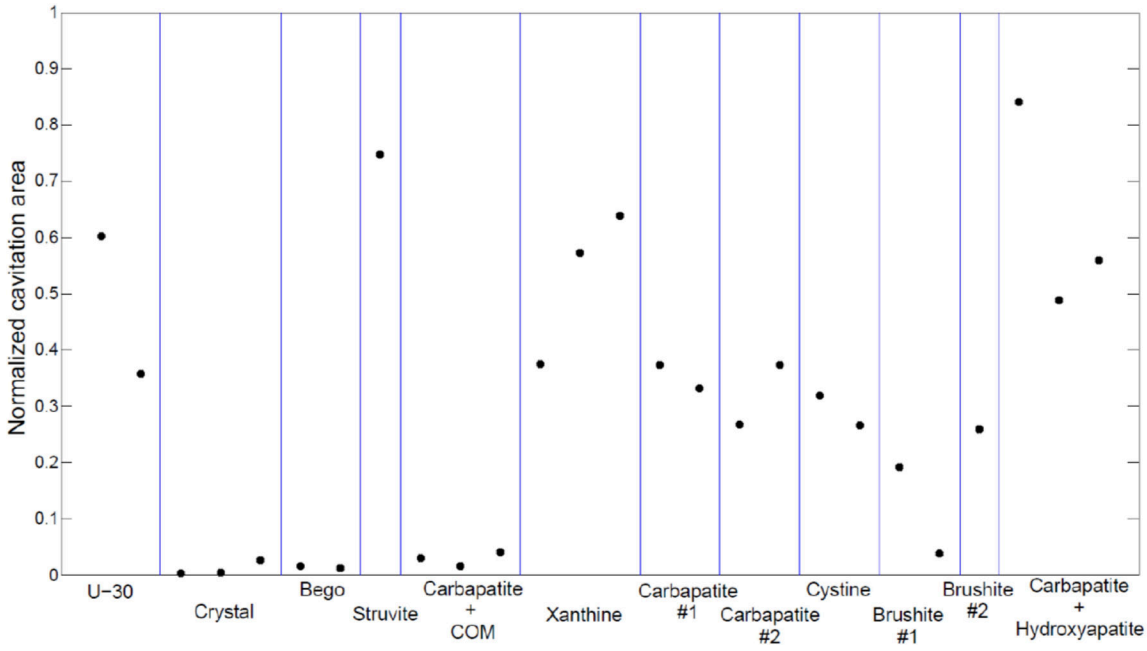

Figure 4:
Cavitation area for all stones tested, sorted by type.

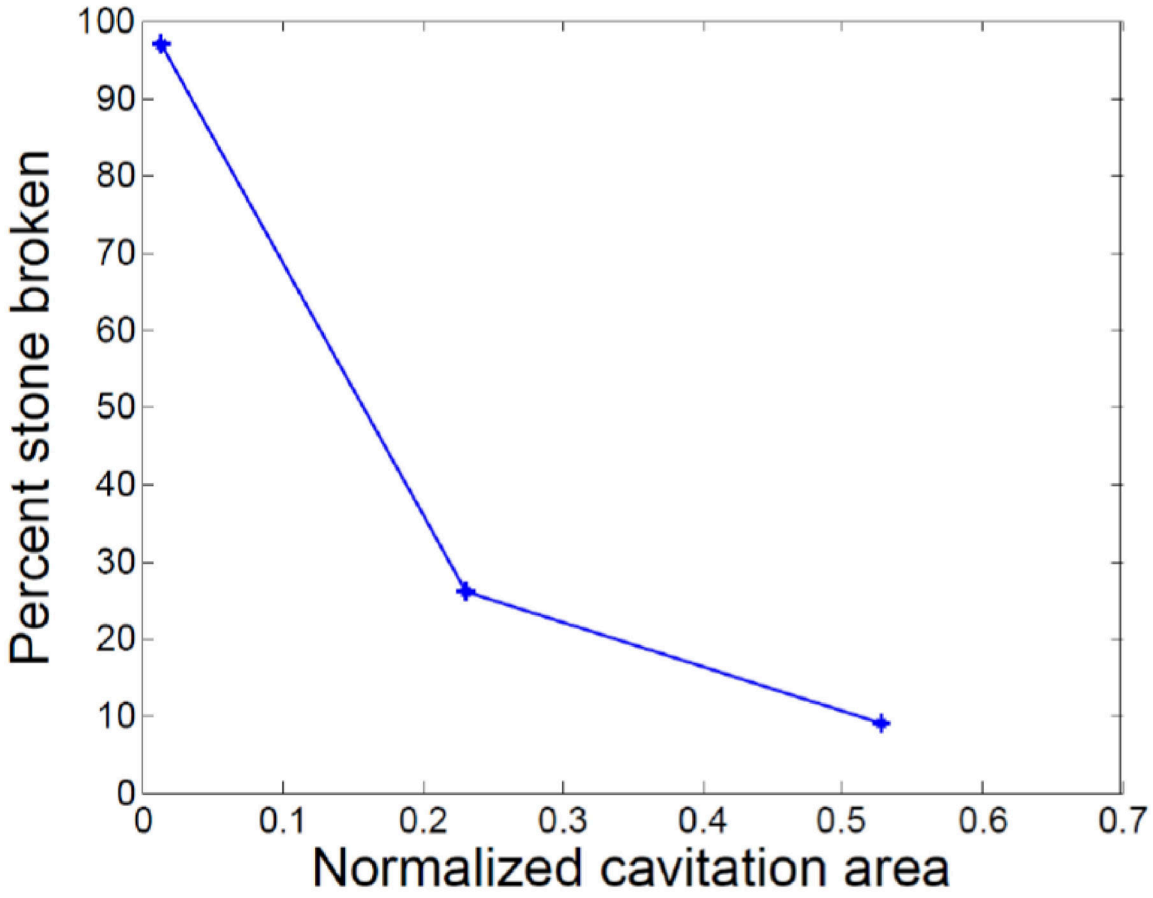

Figure 5:
Stone fragmentation as a function of normalized cavitation area proximal to the stone.